A Millimeter-Wave Microslab™ Oscillator

H. BRIAN SEQUEIRA, MEMBER, IEEE, JOSEPH A. MCCLINTOCK, MEMBER, IEEE,
BRIAN YOUNG, AND TATSUO ITOH, FELLOW, IEEE

Abstract—**Simplified and rigorous mode-matching analyses are applied to find the propagating characteristics of Microslab—a novel, planar waveguiding medium. We also report, for the first time, the coupling of a millimeter-wave GaAs Gunn device *directly* to Microslab using a monolithic-like structure to produce 0.25 mW of oscillator power at 141 GHz.**

I. Introduction

MICROSLAB [1] derives its name from *micro*strip and dielectric *slab* waveguide because it embodies their transmission properties. Fig. 1 illustrates the geometry and permittivities of the structure. The dielectrics and their thicknesses are chosen such that the propagating energy is in a single mode confined to the central dielectric ϵ_g at the upper end of the design frequency range. Near and at this frequency edge, the coupling to the metal conductors is via the evanescent tails of the propagating mode. The metallization improves binding of the wave and suppresses coupling to the laterally leaky slab modes discussed by Peng and Oliner [2]. The reduced field strength at the conductors also reduces ohmic losses.

Coupling to the conductors is stronger at lower frequencies, where ohmic losses are low. Furthermore, this increased coupling causes the mode to become increasingly microstrip-like in nature, thereby lowering dispersion below that of a slab waveguide. Judicious choice of dielectric materials and geometry can produce wide-band, single-mode propagation with low loss and low dispersion. A qualitative and quantitative relationship between the single-mode frequency range and the dimensions and permittivities will become apparent in our discussion below.

To emphasize monolithic feasibility, we constructed a Microslab structure (Fig. 1) using a semi-insulating, single-crystal ⟨100⟩-oriented GaAs substrate of thickness h and permittivity ϵ_g. A grounded alumina slab with permittivity ϵ_s and thickness d_s and a metallized alumina rod of width w and thickness d_l formed the remaining elements of the structure. A comparison of the dimensions of Microslab (Fig. 1) and microstrip [3] for the same range of operating frequencies would intuitively suggest a higher quality factor Q for the former because of the much larger volume-to-surface ratio.

Manuscript received March 29, 1986; revised June 20, 1986.

H. B. Sequeira and J. A. McClintock are with Martin Marietta Laboratories, 1450 S. Rolling Rd., Baltimore, MD 21227-3898.

B. Young and T. Itoh are with the Department of Electrical and Computer Engineering, University of Texas, Austin, TX 78712.

IEEE Log Number 8610552.

Microslab is a trademark of Martin Marietta Corporation.

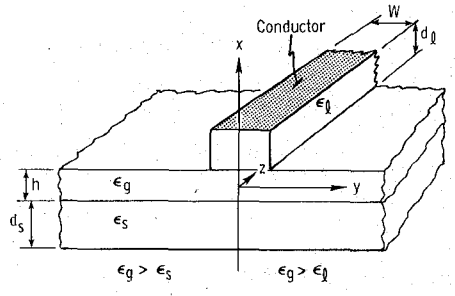

Fig. 1. The Microslab structure.

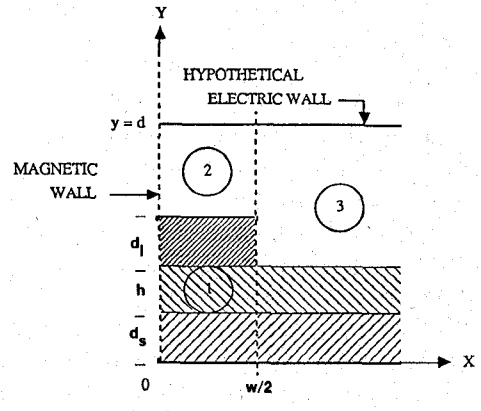

Fig. 2. Structure for analysis.

For convenience, the symbols used in Fig. 1 are summarized below, with the actual materials used in this investigation indicated in parentheses:

- ϵ_s permittivity of the grounded dielectric substrate (Al_2O_3),
- d_s thickness of grounded dielectric slab,
- ϵ_g permittivity of the guiding slab (GaAs),
- h thickness of the guiding slab,
- ϵ_l permittivity of the dielectric loading rod (Al_2O_3),
- d_l thickness of the dielectric loading rod,
- w width of loading rod.

II. Approximate Analysis

Useful insight into the origins of Microslab's favorable transmission properties can be gained from considering a wide-strip approximation for the dominant and higher order modes. For example, such an analysis leads to a closed-form expression for the loss in terms of the surface resistance R_s of the conductors according to the relation

$$\alpha = \frac{1}{\sqrt{\epsilon_{\text{eff}}^r}} \frac{R_s}{\eta} \frac{F}{\epsilon_0} \tag{1}$$

0018-9480/86/1200-1333$01.00 ©1986 IEEE

where η is the intrinsic impedance of free space, superscript r denotes relative permittivity and $F = F(\epsilon_g, \epsilon_s, \epsilon_l, h, d_s, d_l)$ is a form factor, which for wide strips is given by

$$F = \frac{\operatorname{sech}^2(p_s d_s) + \operatorname{sech}^2(p_l d_l)}{\left[\frac{h}{\epsilon_g}\left(\sec^2(qh/2) + \frac{\tan(qh/2)}{(qh/2)}\right) + \frac{d_s}{\epsilon_s}\left(\operatorname{sech}^2(p_s d_s) + \frac{\tanh(p_s d_s)}{(p_s d_s)}\right) + \frac{d_l}{\epsilon_l}\left(\operatorname{sech}^2(p_l d_l) + \frac{\tanh(p_l d_l)}{(p_l d_l)}\right)\right]}. \quad (2)$$

Here p_s, p_l, and q are the transverse propagation factors in materials ϵ_s, ϵ_l, and ϵ_g, respectively, and are obtained by solving the characteristic equations

$$(qh)\tan(qh/2) = \frac{(p_s h)\tanh(p_s d_s)}{\epsilon_g/\epsilon_s} = \frac{(p_l h)\tanh(p_l d_l)}{\epsilon_g/\epsilon_l} \quad (3)$$

in conjunction with conditions imposed by the wave equation

$$(p_s h)^2 + (qh)^2 = (k_0 h)^2(\epsilon_g - \epsilon_s)/\epsilon_0$$
$$(p_l h)^2 + (qh)^2 = (k_0 h)^2(\epsilon_g - \epsilon_l)/\epsilon_0 \quad (4)$$

where k_0 is the free-space wavenumber and ϵ_0 is the free-space permittivity. Note that F has the dimensions of capacitance per unit area, and when $d_s = d_l = 0$, eq. (1) reduces to an expression for loss in a wide microstrip line [4], [5], as expected. For nonzero values of d_s and d_l, F decreases monotonically with increasing values of d and increasing frequency, leading to lower loss. Also, ϵ^r_{eff} increases with frequency owing to stronger confinement of the propagating energy within the central slab (Fig. 5), resulting in a further reduction of the ohmic loss with increasing frequency. We have neglected both radiation loss, because it is low [1], and dielectric loss, because estimates based on our measurements of Microslab loss and those of Afsar [6] indicate that it is small.

The characteristic impedance Z_c obtained from a power–voltage definition in this wide-strip limit is given by

$$Z_c = \eta \frac{F}{\epsilon_0}\frac{\sqrt{\epsilon^r_{\text{eff}}}}{w} 2\frac{\left[\frac{h}{\epsilon^r_g}\frac{\tan qh/2}{qh/2} + \frac{d_s}{\epsilon^r_s}\frac{\tanh(p_s d_s)}{p_s d_s} + \frac{d_l}{\epsilon^r_l}\frac{\tanh(p_l d_l)}{p_l d_l}\right]^2}{\operatorname{sech}^2(p_s d_s) + \operatorname{sech}^2(p_l d_l)}. \quad (5)$$

The superscript r denotes permittivities relative to free space. Again, this expression reduces to that of a wide microstrip when $d_s = d_l = 0$. Although the foregoing discussion gives useful insight, detailed quantitative analysis can be obtained only from a more rigorous mode-matching analysis, presented below.

III. Rigorous Formulation

Analysis by the mode-matching method requires a closed structure, but adding a plate above the Microslab structure at $y = d$ (Fig. 2) discretizes the eigenvalue spectrum. Computation becomes tractable thereby, and choosing a large enough d can minimize the effect of the cover plate. Because the dominant mode has even symmetry about the central vertical plane bisecting the structure, a vertical magnetic wall is placed at $x = 0$ to eliminate the odd modes.

The structure is further subdivided into three regions: region 1 under the strip, region 2 above the strip, and region 3 external to the strip (Fig. 2). The fields in each region are expanded in terms of hybrid TE and TM modes, which satisfy all the required boundary and radiation conditions, and the field expansions are then matched at $x = w/2$. Imposing orthogonality eliminates the expansion coefficients from regions 1 and 2 and leads to an infinite-dimensional homogeneous matrix equation which has a nontrivial solution for the propagation constant β when the determinant of the matrix vanishes.

For computer implementation, the matrix is truncated, yielding an approximate solution that converges to the exact solution in the limit. The number of expansion terms in each region is chosen in proportion to the physical dimensions of the region in the y direction in order to satisfy the edge condition at $x = w/2$ and $y = d_s + h + d_l$.

A rough check for the mode-matching solution can be obtained from an effective-dielectric-constant method, where the top strip is extended to infinity in the y direction, and the resulting slab waveguide of Fig. 3 is analyzed for the lowest TE^x effective dielectric constant $\epsilon_{l\text{eff}}$. The top dielectric strip of Microslab is replaced by an infinite slab with permittivity $\epsilon_{l\text{eff}}$ leading to the hypothetical structure of Fig. 4. This structure is expected to approximate the Microslab since $\epsilon_{l\text{eff}}$ includes the effect of the discontinuity from ϵ_l to air at $x = w/2$. The new structure is then analyzed by the spectral-domain method [7] using one basis function each for the current in the x and z directions.

Results of computation by the mode-matching and effective-dielectric-constant methods are displayed in Fig. 5 for the case $d_s = d_l = 0.25$ mm, $h = 0.33$ mm, $\epsilon_s = \epsilon_l = 9.7\epsilon_0$, $\epsilon_g = 12.9\epsilon_0$, and $w = 0.25$ mm.

IV. Circuit Design

The circuit design (Fig. 6) was deliberately constrained so that the Gunn diode chip within the package was in the plane of one of the GaAs faces of the Microslab structure (to closely approximate the monolithic situation). A reso-

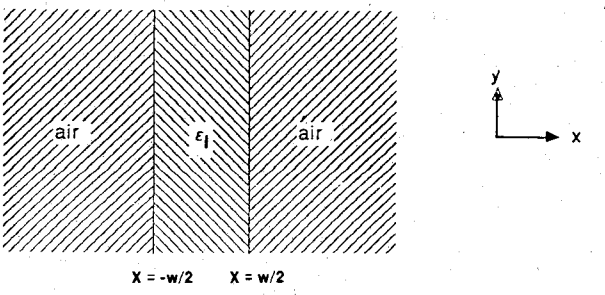

Fig. 3. Structure of the ϵ_l-layer for effective-dielectric-constant analysis.

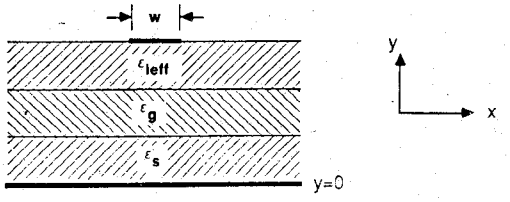

Fig. 4. Approximate equivalent structure derived from analysis of Fig. 3.

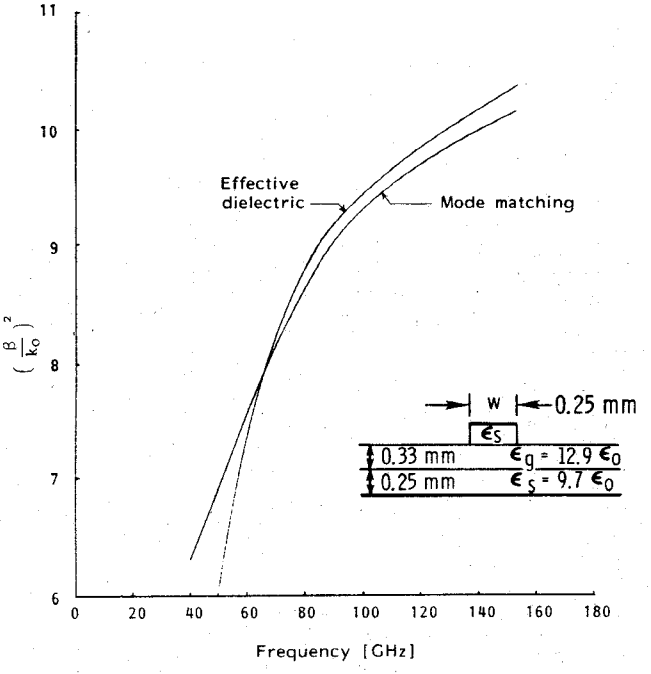

Fig. 5. Dispersion curve for the sample structure (inset).

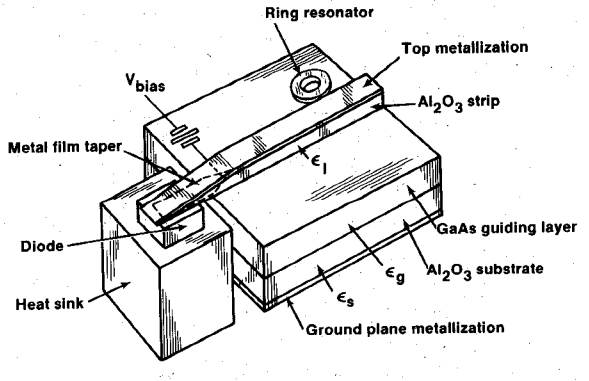

Fig. 6. Millimeter-wave Microslab oscillator circuit.

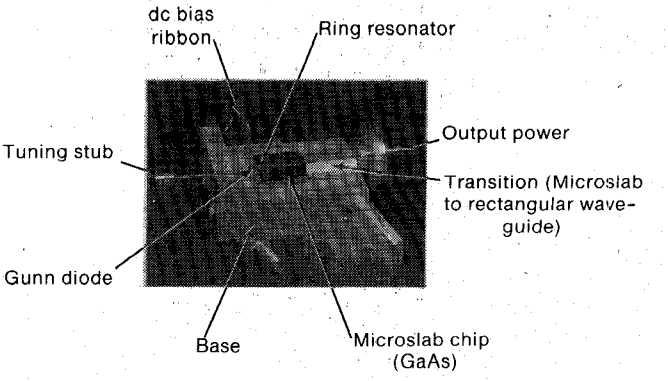

Fig. 7. Partially disassembled millimeter-wave oscillator circuit.

nant ring, 1.27 mm in diameter and 0.25 mm high with a 0.25-mm-thick wall, was positioned alongside the output line (with the same width and height as in Fig. 5) for impedance matching and frequency definition, based on considerations similar to those applied to microstrip DRO oscillators [8]. The final position of the ring and its separation from the Microslab line for maximum output power were determined experimentally.

The oscillator was tested through a cosine-tapered ridge transition to rectangular waveguide [9].

V. Fabrication and Test

The skin depth of millimeter-wave energy at the operating frequency is approximately 0.2 μm. Therefore, the metallized interfaces must be highly polished to realize the low loss. The alumina elements were obtained by grinding and polishing 99.6-percent alumina slabs to the proper thickness and finish, and then cutting and machining them as desired. The parts were then metallized and epoxy-bonded to the vendor-supplied GaAs substrate, and the composite structure was soldered to a gold-plated brass block containing the diode and the waveguide transition. Initially, we designed the circuit to accommodate two resonant rings, one at the fundamental and the other at the second harmonic. However, we modified the design due to difficulties in fabricating these and other elements, and added additional off-chip tuning to produce the actual oscillator circuit shown in Fig. 7.

The Gunn device produced about 0.25-mW power at 141 GHz, corresponding to its third harmonic. The oscillation frequency is in good agreement with the predicted theoretical value of 147 GHz obtained from our mode-matching analysis. The device did not oscillate when the resonant rings were removed, thus demonstrating that the on-chip elements were the primary determinants of circuit behavior. Other oscillator designs and measurements are planned in the future.

VI. Conclusions

We have successfully demonstrated a Gunn oscillator using Microslab, a novel, low-loss, low-dispersion waveguiding medium for millimeter-applications. We believe that this is the first demonstration of *direct* (i.e., without the use of rectangular waveguide or its derivatives) launch-

ing of power into *any* planar dielectric waveguide from a discrete device operating above 90 GHz. Mode-matching and effective-dielectric-constant analyses have been presented which can be used to obtain accurate prediction of the oscillation frequency. Design data from these analyses enable the Microslab propagation constant to be calculated at different operating frequencies. Although we attempted to closely approximate a monolithic design within the fabrication constraints, significant challenges lie ahead. We are concurrently investigating related theory, materials, thermal considerations, and processing requirements necessary for a fully integrated monolithic circuit implementation.

ACKNOWLEDGMENT

The authors thank S. Brown for assembling the oscillator circuit.

REFERENCES

[1] H. B. Sequeira and J. A. McClintock, "Microslab™—A novel planar waveguide for mm-wave frequencies," presented at the 5th Benjamin Franklin Symposium, Philadelphia, PA, May 4, 1985.
[2] S. Peng and A. A. Oliner, "Guidance and leakage properties of a class of open dielectric waveguides: Part I—Mathematical formulations," *IEEE Trans. Microwave Theory Tech.*, vol. MTT-29, pp. 843–854, Sept. 1981.
[3] R. A. Pucel, "Design considerations for monolithic microwave circuits," *IEEE Trans. Microwave Theory Tech.*, vol. MTT-29, pp. 513–534, June 1981.
[4] R. A. Pucel, D. J. Masse, and C. P. Hartwig, "Losses in microstrip," *IEEE Trans. Microwave Theory Tech.*, vol. MTT-16, pp. 342–350, June 1968 (Corrections, vol. MTT-16, p. 1064, Dec. 1968.)
[5] I. J. Bahl and D. K. Trivedi, *Microwaves*, pp. 174, May 1977.
[6] M. N. Afsar, "Dielectric measurements of millimeter-wave materials," *IEEE Trans. Microwave Theory Tech.*, vol. MTT-32, pp. 1598–1609, Dec. 1984.
[7] T. Itoh, "Spectral domain immitance approach for dispersion characteristics of generalized printed transmission lines," *IEEE Trans. Microwave Theory Tech.*, vol. MTT-28, pp. 733–736, July 1980.
[8] M. Dydyk and H. Iwer, "Planar IMPATT diode oscillator using dielectric resonator," *Microwaves & RF*, vol. 23, no. 10, p. 135, Oct. 1984.
[9] D. R. Singh and C. R. Seashore, "Straightforward approach produces broadband transitions," *Microwaves & RF*, vol. 23, no. 9, p. 113, Sept. 1984.

✠

H. Brian Sequeira (S'79–M'82) received the Ph.D. degree in electrical engineering from the University of Delaware in 1982.

He joined Martin Marietta Laboratories after graduation, and has since been involved in millimeter-wave circuit design and testing of semiconductor devices. He invented Microslab and is currently pursuing its development. He is also engaged in monolithic *Ka*-band MESFET and MODFET modeling and testing.

Joseph A. McClintock (M'82) received the Ph.D. degree in physics from The Johns Hopkins University in 1977.

Upon graduation, he joined Martin Marietta Laboratories, where he developed the Labs' MBE growth capability. In the process, he led the development efforts for Schottky barrier mixers, notably the edge-contact mixer and the planar polyisolated mixer for *W*-band applications. He is now developing special-purpose IMPATT diodes for optical injection locking.

✠

Brian Young was born in Dallas, TX, on November 21, 1961. He received the B.S.E.E. from Texas A&M University in 1984. He received the M.S.E.E. from the University of Illinois in 1985, where he was a research assistant in the Ionosphere Radio Research Laboratory. He is currently working towards the Ph.D. degree at the University of Texas at Austin while working as a research assistant in microwave theory.

✠

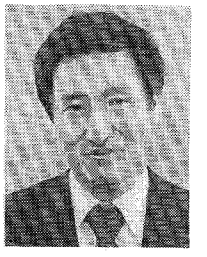

Tatsuo Itoh (S'69–M'69–SM'74–F'82) received the Ph.D. degree in electrical engineering from the University of Illinois, Urbana, in 1969.

From September 1966 to April 1976, he was with the Electrical Engineering Department, University of Illinois. From April 1976 to August 1977, he was a Senior Research Engineer in the Radio Physics Laboratory, SRI International, Menlo Park, CA. From August 1977 to June 1978, he was an Associate Professor at the University of Kentucky, Lexington. In July 1978, he joined the faculty at the University of Texas at Austin, where he is now a Professor of Electrical and Computer Engineering and Director of the Electrical Engineering Research Laboratory. During the summer 1979, he was a guest researcher at AEG-Telefunken, Ulm, Germany. Since September 1983, he has held the Hayden Head Centennial Professorship of Engineering at the University of Texas. In September 1984, he was appointed Associated Chairman for Research and Planning of the Electrical and Computer Engineering Department.

Dr. Itoh is a member of the Institute of Electronics and Communication Engineers of Japan, Sigma Xi, and Commission B of USNC/URSI. He served as the Editor of IEEE TRANSACTIONS ON MICROWAVE THEORY AND TECHNIQUES from 1983 to 1985. He serves on the Administrative Committee of IEEE Microwave Theory and Techniques Society. He is a Professional Engineer registered in the state of Texas.